Food Chemistry: X 27 (2025) 102382

Contents lists available at ScienceDirect

Food Chemistry: X

journal homepage: www.sciencedirect.com/journal/food-chemistry-x

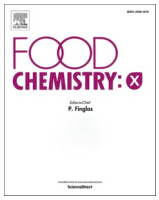

Regulation of corn starch on the properties of tremella polysaccharide-egg white protein-orange juice composite gel and its application in 3D printing

Lili Liu [a,1,*], Beibei Shao [a,1], Wanlin Yang [b], Weiwei Cheng [a], Yue Ding [a], Feng Xiao [a]

[a] College of Food and Bioengineering, National Experimental Teaching Demonstration Center for Food Processing and Security, Henan Engineering Technology Research Center of Food Raw Materials, International Joint Laboratory of Food Processing and Quality Safety Control of Henan Province, Henan Engineering Technology Research Center of Food Microbiology, Henan University of Science and Technology, Luoyang, 471023, PR China

[b] School of instrument Science and Opto-Electronics Engineering, Beijing Information Science and Technology University, Beijing, 100192, PR China

ARTICLE INFO

Keywords:
Food 3D printing
Additive manufacturing
Corn starch
Egg white protein
Rheological properties
Egg white protein EWP corn starch CS Tremella polysaccharide TFP Orange juice OJ

ABSTRACT

The purpose of this paper was to explore the regulation of corn starch (CS) on tremella fuciformis polysaccharide-egg white protein-orange juice (TFP-EWP-OJ) composite gel to develop a new 3D printing material. The results showed that the cylinder of TFP-EWP-OJ composite gel with 0.12 g/mL CS added had the best 3D printing structure and highest printing accuracy. This was an indication that materials with suitable viscosity, hardness, and flowability were more suitable for 3D printing. The nozzle diameter and printing speed were selected to be 1.20 mm and 35 mm/s, respectively. The TFP-EWP-OJ composite gel had greater apparent viscosity and hardness as well as weaker fluidity and a denser network structure with increasing CS concentration. This suggested that the 3D printing performance of TFP-EWP-OJ composite gel can be improved by the incorporation of CS. Furthermore, fourier transform infrared spectroscopy (FT-IR) indicated that no new covalent bonds were formed between CS and the TFP-EWP-OJ composite gel.

1. Introduction

3D printing can customize products and mass production. Its principle is that the pre-designed model structure is printed layer by layer, forming the target product in a stacked manner (Hocine et al., 2020). In the last few years, the development of food 3D printing technology has been rapid because it allows producing personalized food with the advantages of high nutrition, exquisite shape, and specific color. Nowadays, 3D printing technology has been used in research to produce artificial meat (Shi et al., 2023), fat analogue (Lim et al., 2024), and easily swallowed foods (Wang et al., 2023), among other things. As the standard of living improves, people are becoming more and more interested in foods with high nutritional and functionalvalue. Therefore, it make sense to develop some new nutrient-rich inks for 3D printing. This not only satisfies the need for food but also stimulates the taste buds. In short, 3D printing still has a lot of potential for developments.

Protein is a nutrient element essential for the daily life of human beings. Hence, food 3D printing of both plant protein and animal protein has become an important option for researchers. It has been found that pea protein (Lin et al., 2024), soy bean protein (Phuhongsung et al., 2020), whey protein (Li et al., 2024a), and so on can be regarded as the primary materials for food 3D printing. These studies showed that proteins can be used as a key ingredient in food 3D printing to create products that were more nutritious and tailored to individual needs. Egg white protein (EWP) is not only rich in a variety of essential nutrients for the human diet, but also has a number of functional characteristics, such as emulsifying, gelling, foaming, and so on (Sheng et al., 2018). However, gel properties of EWP are impacted by many factors, such as pH, ionic strength, and polysaccharides (He et al., 2021). The previous study found that TFP can improve the gel characteristics of EWP gel (Shao et al., 2025). In addition, TFP had the effects of lowering blood glucose, lowering blood lipids, anti-tumor, anti-aging, anti-oxidation, and regulating immune activity (Ma et al., 2021). Therefore, it was hoped to use the TFP-EWP gel to establish a new food 3D printing material with high nutritional and multifunctional properties. With the concept of healthy eating being introduced, people have paid more and more attention to the dietary fiber content of foods in recent years. Therefore, fruits and vegetables rich in vitamins and dietary fiber were also used for food 3D printing. Chen et al. (2021) used a composite of different protein and fruit-vegetable powders for printing and evaluated the printing results

* Corresponding authors at: College of Food and Bioengineering, Henan University of Science and Technology, 471023, Luoyang, China.
E-mail address: yangliuyilang@126.com (L. Liu).

[1] Lili Liu and Beibei Shao contributed equally to this work.

https://doi.org/10.1016/j.fochx.2025.102382
Received 28 October 2024; Received in revised form 27 January 2025; Accepted 14 March 2025
Available online 19 March 2025

and sensory properties. Xu et al. (2025) developed a new food 3D printing ink using modified pea protein and strawberry powder to meet the dietary requirements of people with dysphagia. In order to enrich the nutritional components of the TFP-EWP gel, orange juice (OJ) was used as the liquid component in the production process of 3D printing material.

The TFP-EWP-OJ composite gel was directly used for 3D printing, the printed products lacked a delicate geometrical shape and supporting capabilities. However, the extrusion performance and ductility of TFP-EWP-OJ composite gel can be improved by adding gelling agent to meet the material requirements of 3D printing process. At present, the gelling agents used for protein-based 3D printing were mainly some edible gums, such as xanthan gum (Liu et al., 2023), carrageenan (Liu et al., 2024), konjac gum (Zhu et al., 2023), and so on. However, these gelling agents generally belonged to food additives and had limited requirements in the food production process. Due to the different printing materials, it may be necessary to add more edible glue to achieve the best printing effect. This violated the provisions of food safety and may had an impact on the health of people. Starch is a natural multifunctional polymer and an important source of energy in the daily diet of human beings (Teixeira et al., 2018). It is composed of amylose and amylopectin. Natural starch has the advantage of being non-toxic, environmentally friendly, renewable, and easy to available (Zhang et al., 2021). It is also an excellent gelling and thickening agent, which can provide the required texture, viscosity, structural properties, and storage stability for food (Wang et al., 2024). However, there has been much done on 3D printing with starch materials, and little has been done on using starch to modulate 3D printing with protein-based materials. Corn starch (CS) was often used in 3D printing due to its good viscoelasticity, low aging properties, and shear thinning properties (He et al., 2021; Liu et al., 2020). For this reason, CS was chosen as the gelling agent for the TFP-EWP-OJ composite gel to make it more suitable for 3D printing.

In this study, the CS and TFP-EWP-OJ composite gel were mixed to prepare raw materials for 3D printing. The optimum concentration of CS was identified by the geometrical shapes and accuracy of the printed samples, and the effects of nozzle diameters and printing speeds on the printing characteristics of TFP-EWP-OJ composite gel were also investigated. In addition, rheology properties, water holding capacity (WHC), texture profile, scanning electron microscopy (SEM), and fourier transform infrared spectroscopy (FT-IR) of the TFP-EWP-OJ composite gel were characterised. The aim of this study was to develop a new 3D printing ink to provide a new idea for improving the printability of protein based materials.

2. Materials and methods

2.1. Materials and reagents

EWP was purchased from Bozhou Haichuan Egg Products Co., Ltd. (Anhui, China). Tremella fuciformis polysaccharide was obtained from Shanxi Nanba Bio-Chemical Co., Ltd. (Shanxi, China). Orange juice was provided by Beijing Huiyuan Food & Beverage Co., Ltd. (Beijing, China). CS (27.54 % amylose content, 72.46 % amylopectin content) was supplied by Shanghai RYON Biotechnology Co., Ltd. (Shanghai, China).

2.2. Preparation of TFP-EWP-OJ composite gel

EWP and TFP were dissolved separately with orange juice in a beaker and were stirred for 2 h at 25 °C. Next, it was placed at 4 °C for 12 h to ensure complete hydration of TFP and EWP. The EWP and TFP solution were mixed and stirred for 1 h after hydration. The final concentrations of EWP and TFP were 0.20 g/mL and 0.03 g/mL, respectively (Shao et al., 2025). The prepared composite solution was water-bathed for 40 min at 90 °C and cooled in an ice water bath immediately after the completion of the water bath. Then, CS(0.00, 0.06, 0.08, 0.10, 0.12, 0.14, 0.16 g/mL) was added to the TFP-EWP-OJ composite gel and stirring at 400 rmp for 5 min to mix well. Finally, TFP-EWP-OJ composite gel containing different concentrations of CS was water bathed at 90 °C for 30 min to allow the CS to fully gelatinize and improve the properties of TFP-EWP-OJ composite gel. During the water bath, a food-grade preservative film was placed around the mouth of the beaker to protect against water loss due to evaporation. After the water bath ended, the prepared TFP-EWP-OJ composite gel samples were cooled in an iced water bath.

2.3. 3D printing process

2.3.1. 3D printing and printing accuracy of the TFP-EWP-OJ composite gel

TFP-EWP-OJ composite gel samples were printed using 3D printer (Food Bot—D1, Shiyin Technology Co., Ltd., Hangzhou, China). The printed model was a cylinder with a 50 % fill density, a diameter of 25 mm, and a height of 15 mm. The nozzle diameter of 1.20 mm was used. The printing speed was set to 25 mm/s and the temperature was set to 25 °C. In addition, the printing accuracy of TFP-EWP-OJ composite gel 3D printing products with different CS concentrations was evaluated by comparing the differences in the diameter and height of the printed cylinder and the model cylinder. Formulas (1) and (2) referred to the deviation of the diameter and height of the printed sample from the diameter and height of the model, respectively. Formula (3) referred to the average deviation of the diameter and height of the printed product. The smaller the average deviation, the higher accurate the printed sample. The formulas were as follows:

$$E_r = |(S_r - T_r)/T_r| \times 100\% \quad (1)$$

$$E_h = |(S_h - T_h)/T_h| \times 100\% \quad (2)$$

$$E_a = (E_r + E_h)/2 \quad (3)$$

Where E_r and E_h are the relative deviations of the diameter and the height, respectively (%). S_r and S_h are the diameter length and height of the printed sample, respectively (mm). T_r and T_h are the design values for the diameter length and height of the model, respectively (%). E_a is the accuracy (%). Formulas applicable scope: $E_a < 100$ %.

2.3.2. 3D printing process with different nozzle diameters and printing speeds

Nozzle diameters and printing speeds were optimized under the optimum CS concentration level. The printed model was also a cylinder with a height of 15 mm and a diameter of 25 mm. When the printing speed was 25 mm/s, the nozzle diameter (0.60, 0.84, 1.20, 1.55, 2.00 mm) was changed for printing. Printing was performed by changing the printing speed (20, 25, 30, 35, 40 mm/s) at the optimum nozzle diameter. In addition, several delicate samples were printed to illustrate the printability of the material.

2.4. Rheological analyses

2.4.1. Apparent viscosity measurement

The rheological properties of the TFP-EWP-OJ composite gel samples were tested using the rheometer (DHR-1, TA Co., US). The distance between the plate and the platform was 1000 μm, and the diameter of the plate was 40 mm. In order to determine the accuracy of the results, the TFP-EWP-OJ composite gel samples were placed and allowed to stand for 2 min prior to the test. The shear rate was adjusted from 0.1 to 100 s^{-1} during testing. Furthermore, the apparent viscosity was described by the Ostwald-de-Waele model. The equation was as follows.

$$\eta = K \times \gamma^{n-1} \quad (4)$$

Where η (Pa·s) is apparent viscosity of TFP-EWP-OJ composite gel samples, K ($Pa \cdot s^n$) is consistency index of TFP-EWP-OJ composite gel samples, γ (s^{-1}) is shear rate during measurement, n is flow behaviour

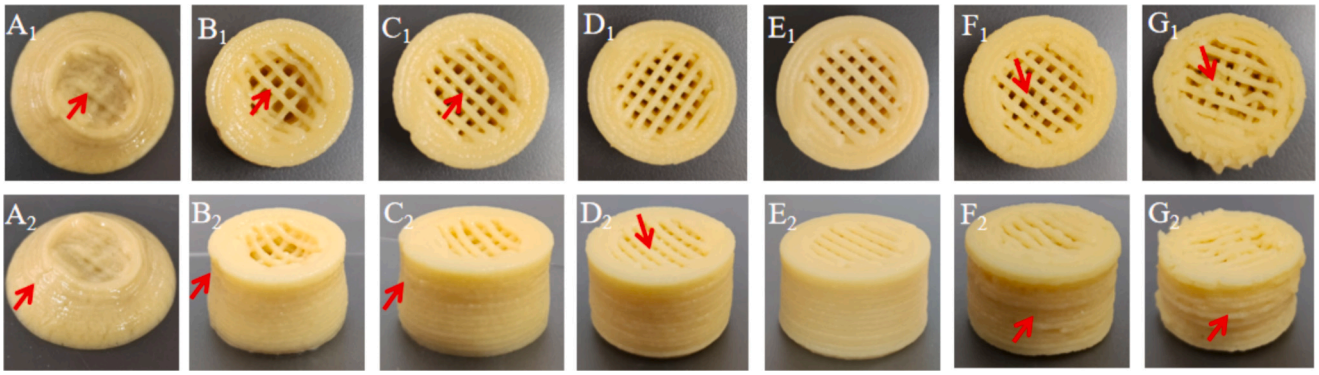

Fig. 1. 3D printed samples with TFP-EWP-OJ composite gel of different CS concentrations at 1.20 mm nozzle diameter and 25 mm/s printing speed. A_1-G_1 were top views of the printed products of TFP-EWP-OJ composite gel at CS concentrations of 0.00, 0.06, 0.08, 0.10, 0.12, 0.14, 0.16 g/mL, respectively. A_2-G_2 were main views of the printed products of TFP-EWP-OJ composite gel at CS concentrations of 0.00, 0.06, 0.08, 0.10, 0.12, 0.14, 0.16 g/mL, respectively. TFP: Tremella polysaccharide, EWP: Egg white protein, OJ: Orange juice, CS: Corn starch.

index of TFP-EWP-OJ composite gel samples.

2.4.2. Dynamic viscoelastic properties measurement

TFP-EWP-OJ composite gel samples were subjected to frequency sweep tests ranging from 0.1 to 100 rad/s (25 °C). The strain value was set at 0.1 %, which was in the linear viscoelastic range. The software equipped with the rheometer was used to record the storage modulus (G′), loss modulus (G″) and tan δ = G″/G′ (loss tangent) of TFP-EWP-OJ composite gel samples.

2.5. WHC analysis

The method of Yu et al. (2023) was used to determine the WHC of the TFP-EWP-OJ composite gel samples with slight modifications. First, the TFP-EWP-OJ composite gel samples (5 g) were laid in a 10 mL centrifuge tube. Then, they were placed in a centrifuge (H1650, Hunan Xiang Instrument Development Co., Ltd., Hunan, China) and centrifuged at 10000*g* for 30 min at 25 °C. After centrifugation, the supernatant was discarded, and the water on the TFP-EWP-OJ composite gel samples surface was sucked off using the filter paper. The centrifuge tube and remaining TFP-EWP-OJ composite gel were weighed. The WHC was calculated as the following equation:

$$WHC = (m_1 - m_0)/(m_2 - m_0) \times 100\% \quad (5)$$

Where m_0 is the weight of the empty centrifuge tube (g), m_1 is the weight of the centrifuge tube and the TFP-EWP-OJ composite gel prior to centrifugation (g), m_2 is the weight of the centrifuge tube and the rest of the TFP-EWP-OJ composite gel (g).

2.6. Texture profile analysis (TPA)

A texture analyser (SMS TA.XT Epress Enhanced, Stable Micro Systems Co., Ltd., USA) was used to determine the TPA of the TFP-EWP-OJ composite gel samples. The experimental parameters were established using the method of Ren et al. (2023) with minor modifications. A probe of P/0.5 was selected for the test. At the start of the test, the probe was lowered at a rate of 5 mm/s. During the test period, the probe was dropped at a rate of 1 mm/s. At the end of the test, the probe was raised at a rate of 5 mm/s. The probe dwell time was 0.5 s, and the sample deformation was 45 %. Each set of TFP-EWP-OJ composite gel samples was tested three times to obtain the textural characterisation curves, recording the hardness, springiness, cohesiveness and gumminess.

2.7. FT-IR analysis

The FT-IR measurement method was based on Azam et al. (2018) method and slightly modified. The TFP-EWP-OJ composite gel samples were freeze dried and examined useing the FT-IR spectrometer (VERTEX70, Bruker Co., Ltd., Germany). The freeze dried TFP-EWP-OJ composite gel samples were mixed well with KBr in a 1:100 mass ratio. Then, the KBr blanks were used as controls. The TFP-EWP-OJ composite gel samples of spectra curves were obtained in the wavenumber range of 4000–400 cm^{-1} at room temperature.

2.8. SEM measurement

Microstructural features of the freeze dried TFP-EWP-OJ composite gel samples were observed by SEM (TM3030Plus, Daojin Co., Ltd., Japan). The measurement was carried out according to a slightly modified version of the method of Li et al. (2024b). Prior to the test, TFP-EWP-OJ composite gel samples were sprayed with gold to obtain the clearer microstructure images. Subsequently, micrographs of the TFP-EWP-OJ composite gel samples were acquired at an polishing voltage of 20 kV.

2.9. Statistical analysis

All experiments were repeated in triplicate to avoid contingency. Analysis of significant differences among the data was by means of SPSS 26 software ($P < 0.05$). Data visualization was performed using Origin 2023 b software.

3. Results and discussions

3.1. 3D printing

3.1.1. 3D printing and printing accuracy of TFP-EWP-OJ composite gel

The 3D printing properties of TFP-EWP-OJ composite gel with different CS concentrations were evaluated using a cylinder. As shown in Fig. 1, printed samples from TFP-EWP-OJ composite gel without addition of CS collapsed almost completely and did not form a cylinder. The printed samples with 0.06 g/mL CS added exhibited poor support, collapsed in the middle, and showed a tendency to shrink at the top and bottom, resulting in unsatisfactory printing results. This may be due to the fact that the material was more fluid and had less support. The printed samples with 0.08 g/mL and 0.10 g/mL CS added had a smaller collapse in the centre and were similar in shape to the model, but there were still some minor deviations. Printed samples with 0.12 g/mL CS added showed smooth lines, complete structure, greater resolution, minimal slumping distortion, and excellent print results. This was attributed to the fact that the fluidity of the material was reduced and the viscoelasticity of the system was increased, which ensured good extrusion characteristics and stability with high fidelity. However, the printed samples containing 0.14 g/mL and 0.16 g/mL CS had inferior

Table 1
Accuracy of 3D printed samples of TFP-EWP-OJ composite gel with different CS concentrations. TFP: Tremella polysaccharide, EWP:Egg white protein, OJ: Orange juice, CS: Corn starch.

CS concentrations (g/mL)	Printing Accuracy (%)
0.06	6.73 ± 0.18^{a}
0.08	4.03 ± 0.19^{b}
0.10	1.11 ± 0.06^{de}
0.12	0.75 ± 0.03^{e}
0.14	1.31 ± 0.05^{d}
0.16	2.66 ± 0.20^{c}

Different lowercase letters mean significant difference among respective series at $P < 0.05$.

print outcomes, and the printed samples showed poor line extrusion and breaking, as well as an uneven surface, during the printing process. This was caused by the concentrations of too high CS, which made the materials less fluid, harder, and more difficult to extrude.

The accuracy of the TFP-EWP-OJ composite gel printed samples was shown in Table 1. The smaller the average deviation of the printed samples, the higher the accuracy. The TFP-EWP-OJ composite gel without CS did not print a shape similar to a cylinder, so its accuracy was not calculated. As can be seen in Table 1, the accuracy of the printed samples improved. This may be due to the fact that the hardness and viscoelasticity of the TFP-EWP-OJ composite gel were improved by the increase in CS concentration. However, the printing accuracy of printed samples containing 0.14 g/mL and 0.16 g/mL CS dropped. This could be because the printing materials with high hardness and viscoelasticity were difficult to extrude. In summary, the 3D printing effect of TFP-EWP-OJ composite gel with the concentration of 0.12 g/mL CS was found to be the optimal.

3.1.2. *Optimisation of the nozzle diameter and printing speed*

The accuracy and surface roughness of the printed samples were

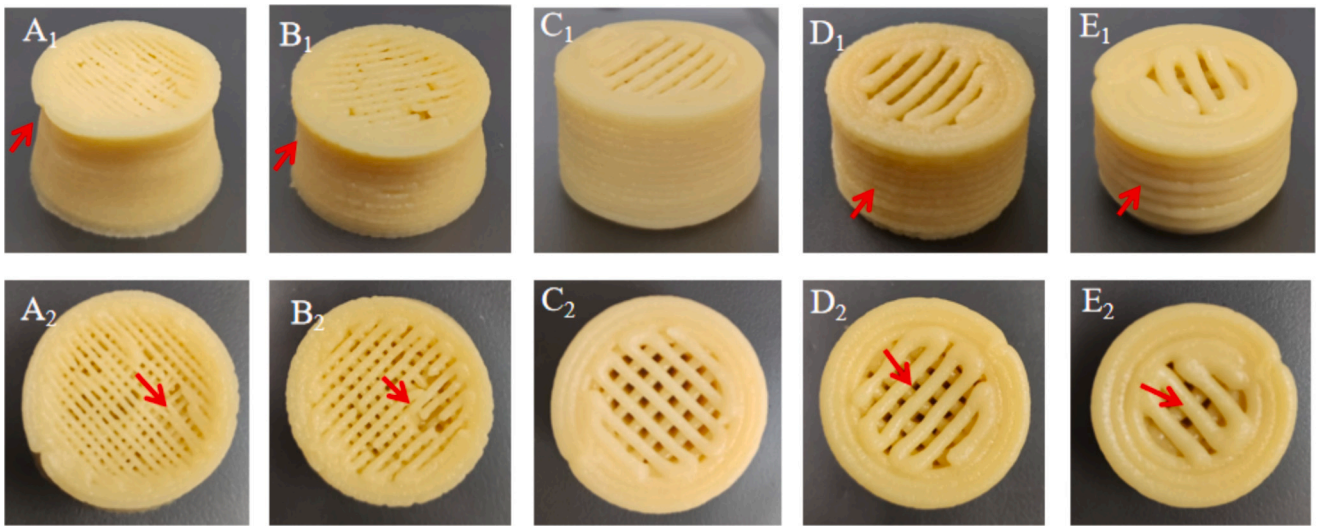

Fig. 2. Printed samples with different nozzle diameters at TFP-EWP-OJ composite gel of 0.12 g/mL CS concentration and 25 mm/s print speed. A_1-E_1 were top views of the printed products of TFP-EWP-OJ composite gels at a nozzle diameter of 0.60, 0.84, 1.20, 1.55, 2.00 mm, respectively. A_2-E_2 were main views of the printed products of TFP-EWP-OJ composite gels at a nozzle diameter of 0.60, 0.84, 1.20, 1.55, 2.00 mm, respectively. TFP: Tremella polysaccharide, EWP: Egg white protein, OJ: Orange juice, CS: Corn starch.

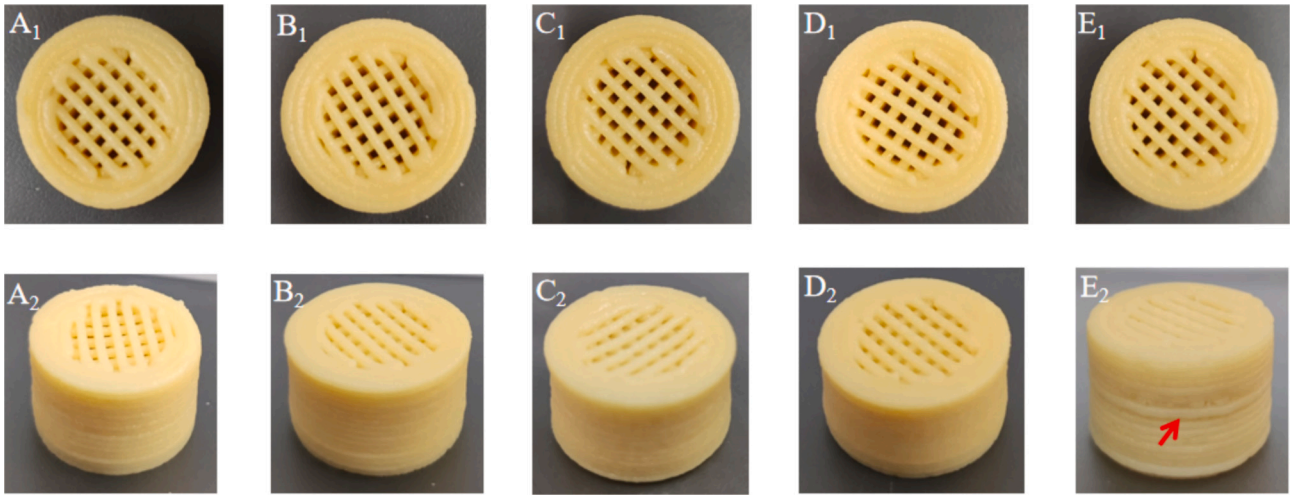

Fig. 3. Printed samples with different print speeds at TFP-EWP-OJ composite gel of 0.12 g/mL CS concentration and 1.20 mm nozzle diameter. A_1-E_1 were top views of the printed products of TFP-EWP-OJ composite gels at a at a print speeds of 20, 25, 30, 35, 40 mm/s, respectively. A_2-E_2 were main views of the printed products of TFP-EWP-OJ composite gels at a nozzle diameter of 20, 25, 30, 35, 40 mm/s, respectively. TFP: Tremella polysaccharide, EWP: Egg white protein, OJ: Orange juice, CS: Corn starch.

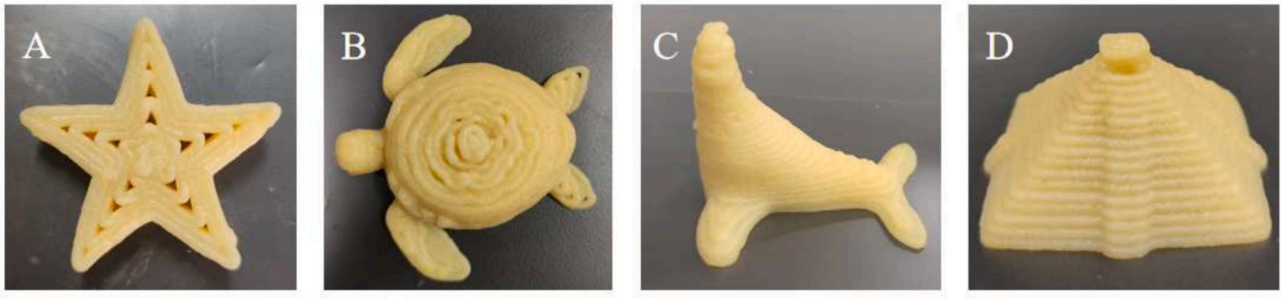

Fig. 4. some samples of beautifully patterned printed at TFP-EWP-OJ composite gel with 0.12 g/mL CS concentration, 1.20 mm nozzle diameter, and 35 mm/s printing speed. (A. Five pointed star, B. Turtle, C. Seal, D, Pyramid) TFP: Tremella polysaccharide, EWP: Egg white protein, OJ: Orange juice, CS: Corn starch.

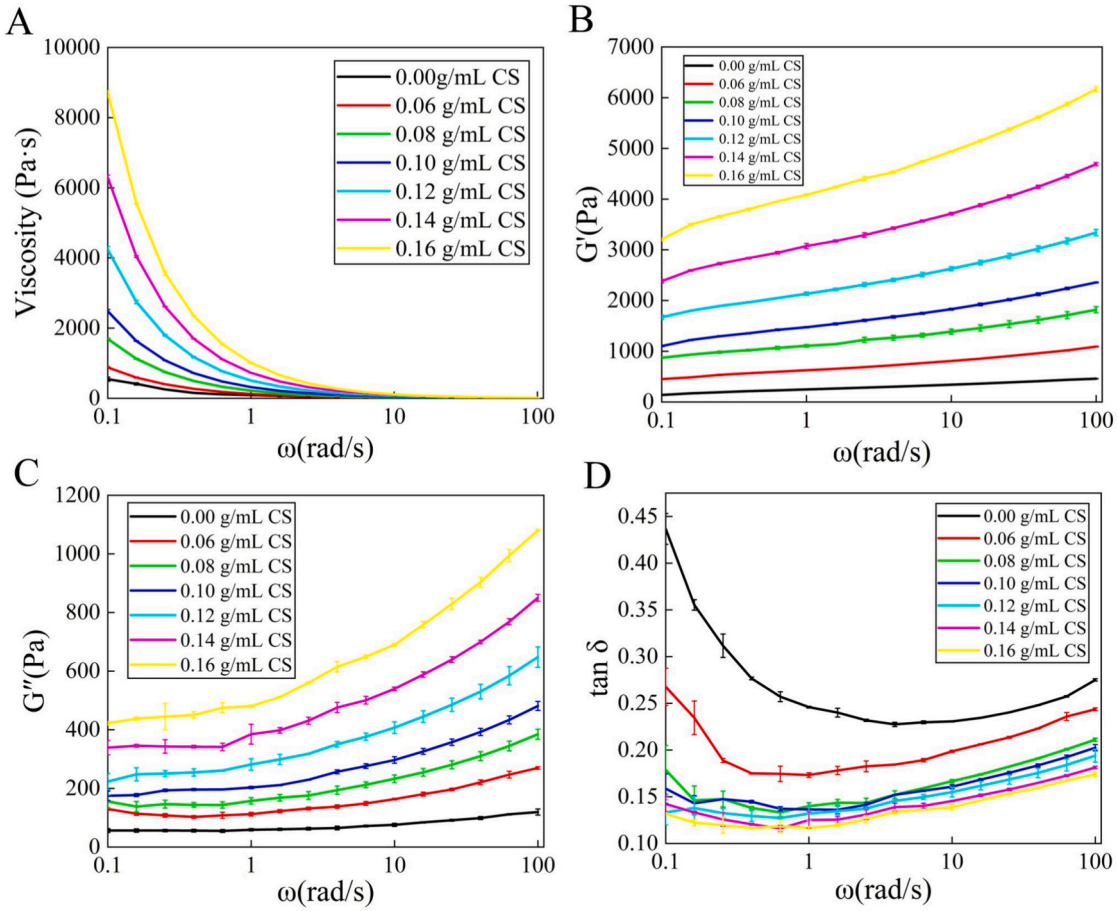

Fig. 5. Effect of different CS concentrations on apparent viscosity (A), storage modulus (B) and loss modulus (C), tan δ (D) of TFP-EWP-OJ composite gel. CS: Corn starch, TFP: Tremella polysaccharide, EWP: Egg white protein, OJ: Orange juice.

affected by the size of the nozzle diameters. The optimum diameter of the print nozzle will vary depending on the materials to be printed. The printed samples of TFP-EWP-OJ composite gel with different nozzle diameters were shown in Fig. 2. When the nozzle diameter was 0.60 mm, the material was not extruded smoothly, resulting in a collapse in the middle of the printed samples and a change in shape. There was a slight tendency to shrink in the middle of the 0.84 mm nozzle diameter printing samples, and the printing effect were poor. The printed samples with a nozzle diameter of 1.20 mm had a delicate geometrical shape and stability. Although the printed samples with nozzle diameters of 1.55 mm and 2.00 mm had good stability, the geometrical shapes were not delicate enough due to the thicker printed lines. For this reason, a nozzle diameter of 1.20 mm was selected for the 3D printing of the TFP-EWP-OJ composite gel.

As shown in Fig. 3, printed samples at different printing speeds were displayed. The geometrical shapes of the printed samples were not much different at different printing speeds. When the printing speed was 40 mm/s, there were lines of different thickness in the middle of the printed product, which led to the decrease of the accuracy of the printed product and affected the overall appearance. However, printing speed was directly proportional to the print efficiency. Considering the printing efficiency and printing quality, the 35 mm/s printing speed was used for 3D printing. Furthermore, as illustrated in Fig. 4, some of the more complex and sophisticated models were printed. This can stimulate the appetite of people, improve eating pleasure, and improve the value of food 3D printing.

Table 2
Ostwald-de-Waele model parameters K, n from equation of TFP-EWP-OJ composite gel with different CS in concentrations. K: consistency index, n:flow behaviour index, TFP: Tremella polysaccharide, EWP:Egg white protein, OJ: Orange juice, CS: Corn starch.

CS concentrations (g/mL)	K(Pa·s)	n	R^2
0.00	83.76 ± 6.47^{g}	0.1771 ± 0.0061^{a}	0.9934
0.06	125.09 ± 3.99^{f}	0.1539 ± 0.0037^{a}	0.9999
0.08	219.06 ± 4.51^{e}	0.1118 ± 0.0045^{b}	0.9999
0.10	317.55 ± 2.93^{d}	0.1086 ± 0.0115^{b}	0.9999
0.12	502.31 ± 3.69^{c}	0.0752 ± 0.0057^{c}	0.9999
0.14	715.65 ± 5.37^{b}	0.0574 ± 0.008^{c}	0.9999
0.16	976.52 ± 2.60^{a}	0.0518 ± 0.0042^{c}	0.9998

Different letter above the same column indicate a significant difference ($P < 0.05$).

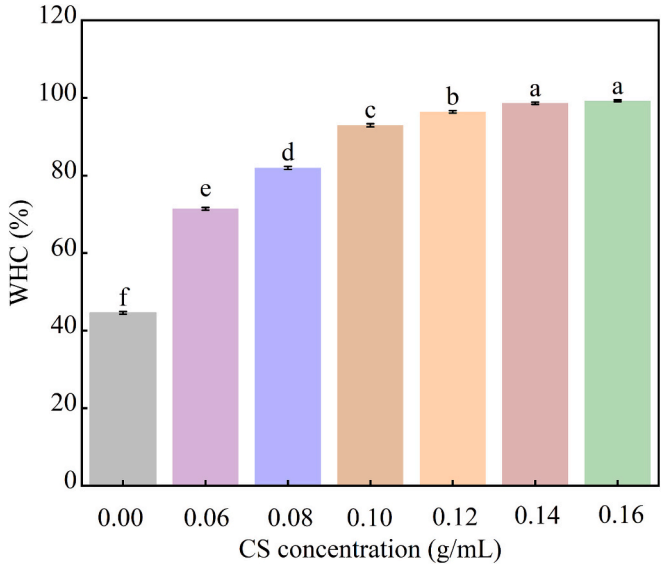

Fig. 6. Effect of different CS concentrations on WHC of TFP-EWP-OJ composite gel. Values with different letters are significantly different ($P < 0.05$). CS: Corn starch, WHC: Water holding capacity, TFP: Tremella polysaccharide, EWP: Egg white protein, OJ: Orange juice.

3.2. Rheological characterisation of TFP-EWP-OJ composite gel

3.2.1. Apparent viscosity

Rheological properties were significant indexes to assess for 3D printing of food inks. Inks used for food 3D printing should have an appropriate apparent viscosity. The apparent viscosity of the printed inks should be low enough to allow them to extrude smoothly from the nozzle. It must also be high enough to remain stable on the printing platform after the food inks were extruded (Liu et al., 2019). As shown in Fig. 5A, the apparent viscosity of the TFP-EWP-OJ composite gel samples with different CS concentrations was gradually reduced with increasing shear rate. This suggested that the TFP-EWP-OJ composite gel samples were typically pseudoplastic fluids with shear-thinning characteristics. It was favorable that the TFP-EWP-OJ composite gel can be more easily extruded. It also made a contribution to the rapid structural recovery of the printed material after deposition, ensuring the fidelity and stability of the printed structures (Zheng et al., 2024). Meanwhile, The apparent viscosity of TFP-EWP-OJ composite gel increased significantly with the increase of CS concentrations. Out of all of them, the apparent viscosity of TFP-EWP-OJ composite gel reached the maximum value of 8754 Pa.s at a CS concentration of 0.16 g/mL. This occurred because there were more chains in each space, which encouraged chain cross-linking and created a denser network structure with thicker walls and smaller cell sizes (Liu et al., 2018a). Macroscopically, this manifested itself as an increase in the consistency and apparent viscosity of the system.

To investigate the relationship between shear rate and apparent viscosity of TFP-EWP-OJ composite gel samples more comprehensively, the experimental data were fitted using Origin 2023 b software based on the Ostwald-Dwyer equation. The specific results were shown in Table 2. The correlation coefficients (R^2) for all TFP-EWP-OJ composite gel samples were greater than 0.99. This was an indication of a good fit for all data. The K value of the TFP-EWP-OJ composite gel gradually increased as the concentration of the CS increased. It was further illustrated that the apparent viscosity of TFP-EWP-OJ composite gel was improved due to the addition of CS. This also showed that as the concentration of CS increased, the material became less extrudable and harder to extrude out from the nozzle when printing. In addition, the value of n was less than one for all samples, revealing that all the samples exhibited shear thinning characteristics. A higher apparent viscosity contributed to maintaining the shape of the printed samples and improved the phenomenon of broken stripes during the printing process. If the apparent viscosity was too high, the printing material will be difficult to squeeze out from the nozzle and print accuracy will be reduced. Therefore, the appropriate apparent viscosity was one of the key determinants for the success of 3D printing.

3.2.2. Dynamic viscoelastic properties

G' is a reflection of the elastic behaviour and mechanical intensity of the material. The high level of mechanical intensity of the materials revealed outstanding support ability and were less prone to collapse, which effectively maintained the stability of the printed models (Liu et al., 2018a). G″ denotes the viscous behaviour of the samples, which reflects the energy consumed by the material throughout the deformation process as a result of viscous deformation (Liu et al., 2018b). Fig. 5B and C shown that both G' and G″ of the TFP-EWP-OJ composite gel exhibited a gradual increase with the concentration of CS. Moreover, the G' and G″ of the TFP-EWP-OJ composite gel reached a maximum value of 6132.54 Pa and 1077.61 Pa at a CS concentration of 0.16 g/mL, respectively. This may be due to the swelling of the starch granules during the heating process, resulting in the release of the amylose within the structure to act as a structural filler (Nailín et al., 2023). G' values for all TFP-EWP-OJ composite gel samples were uniformly greater than G″ over the measured range. This indicated that the printed materials displayed predominantly elastic behaviour within the measured frequencies. These elastic structures maintained relative stability under external forces and enhanced resistance to deformation between layers as the printed products were deposited on the printing platform. In general, materials with higher G' and G″ values were more suitable for 3D printing. This was because the materials displayed superior shape retention and could be bonded to the previous layer following extrusion, thereby resulting in a more robust internal structure of the printed samples (Costakis et al., 2016). However, the G' value was too large, which will lead to the difficulty of extrusion of printing materials and not benefit the 3D printing. This was the reason why the print effect of the TFP-EWP-OJ composite gel printed products with 0.12 g/mL CS was the better, while the printed products of 0.14 g/mL and 0.16 g/mL CS were worse (Fig. 1).

Furthermore, the viscoelasticity of the materials can be quantified by the loss tangent ($\tan\delta = G''/G'$). If $\tan\delta > 1$, it indicated that the material exhibited predominantly viscous characteristics. If $\tan\delta < 1$, it indicated that the material exhibited predominantly elastic characteristics. Moreover, the greater the tan δ value, the stronger the fluidity of the material and the more inclined it was to be liquid. The smaller the tan δ value, the weaker the fluidity of the material and the more inclined it was to be solid (An et al., 2023). The tan δ of each sample was found to decrease at first, followed by an increase, and it was less than 1, as shown in Fig. 5D. This indicated that the TFP-EWP-OJ composite gel samples all exhibited elastic behaviour. In addition, tan δ gradually

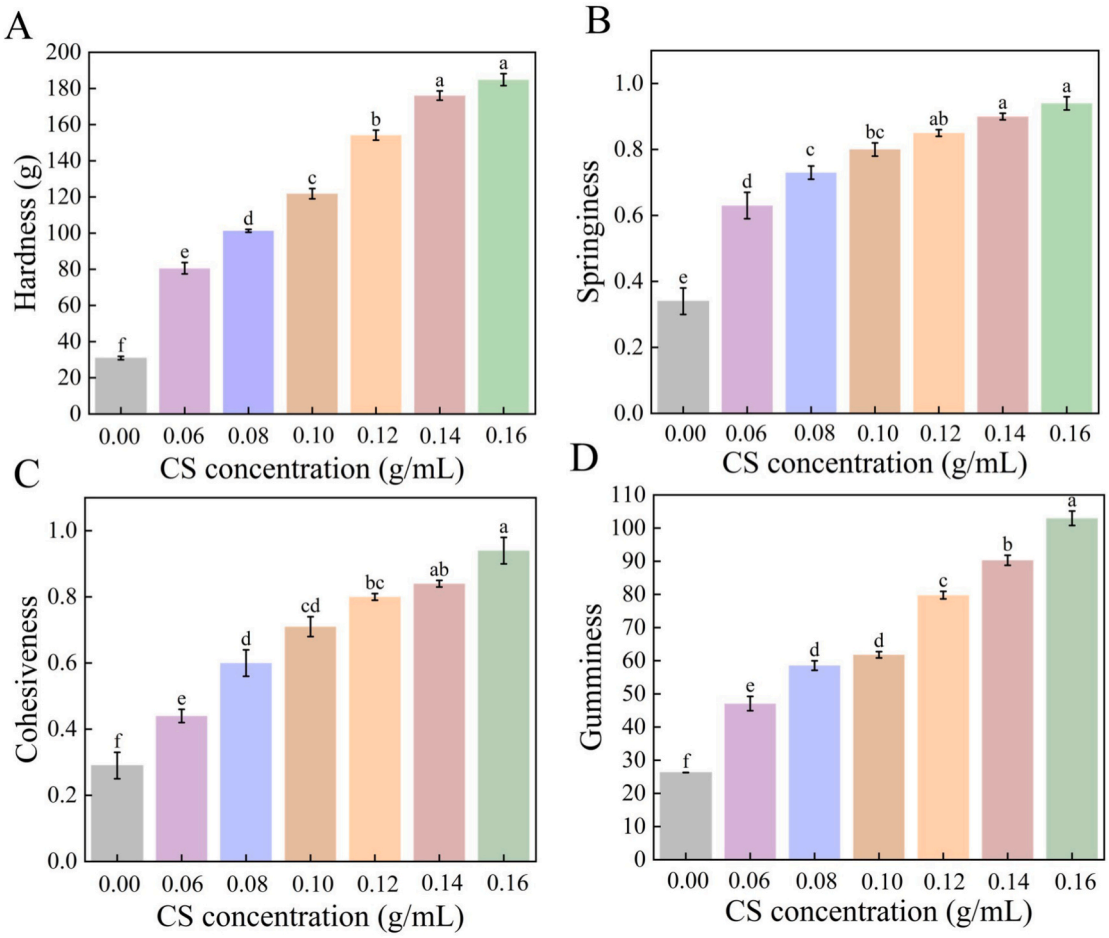

Fig. 7. The effect of different CS concentrations on the texture properties of TFP-EWP-OJ composite gel. (A): hardness, (B): springiness, (C): gumminess, (D): cohesiveness. Values with different letters are significantly different ($P < 0.05$). CS: Corn starch, TFP: Tremella polysaccharide, EWP: Egg white protein, OJ: Orange juice.

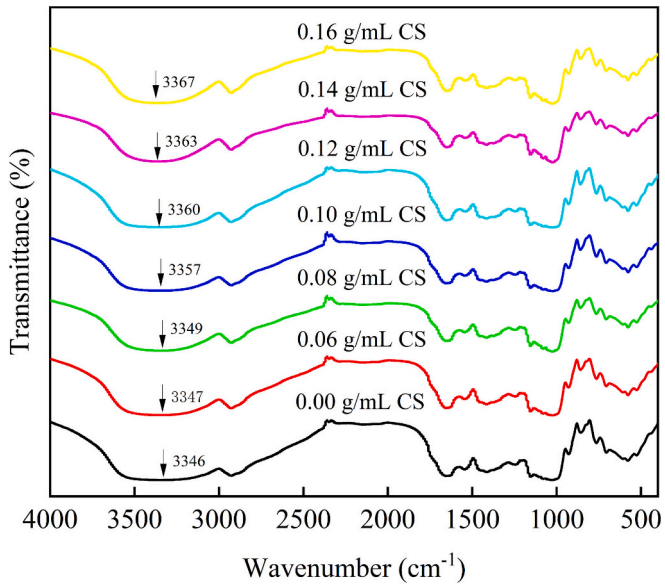

Fig. 8. FT-IR of TFP-EWP-OJ composite gel with different CS concentrations. FT-IR Fourier Transform Infrared Spectroscopy, TFP: Tremella polysaccharide, EWP: Egg white protein, OJ: Orange juice, CS: Corn starch.

decreased with the increase of CS concentration. This meant that the TFP-EWP-OJ composite gels become poor in fluidity and gradually exhibit solid-like behaviour. This can lead to phenomena such as difficulty in extruding the print material and broken print lines. This was consistent with the results of the 3D printing.

3.3. WHC

WHC is associated with the structural and sensory properties of the gel (Pan et al., 2021). The greater the WHC of the gel, the less likely it was that the water within the gel would be expelled when subjected to external pressure, thereby enhancing the stability of the printed products. As shown in Fig. 6, the WHC of the TFP-EWP-OJ composite gel increased significantly ($P < 0.05$) as the concentration of CS increased and reached a maximum of 99.27 % at a concentration of 0.16 g/mL. This may be due to the fact that water not tightly bound to the TFP-EWP-OJ composite gel network was absorbed with CS in the gelatinization process. Furthermore, the more CS was added, the more water was absorbed and the better the filling effect on the protein network structure, making the structure more compact and increasing its ability to bind water (Hu et al., 2023). The printed materials with too low WHC will exhibit more liquid behaviour, resulting in incomplete print product form and collapse (Fig. 1 A_1, $1A_2$, $1B_1$, $1B_2$, $1C_1$, and $1C_2$). As the WHC increased, the flow of the print material weakened, the viscosity increased, and the printed lines became more self-supporting (Fig. 1 D_1, $1D_2$, $1E_1$, and $1E_2$). However, the excessively high WHC can cause poor flow of the printed material to the point of clogging the nozzle and

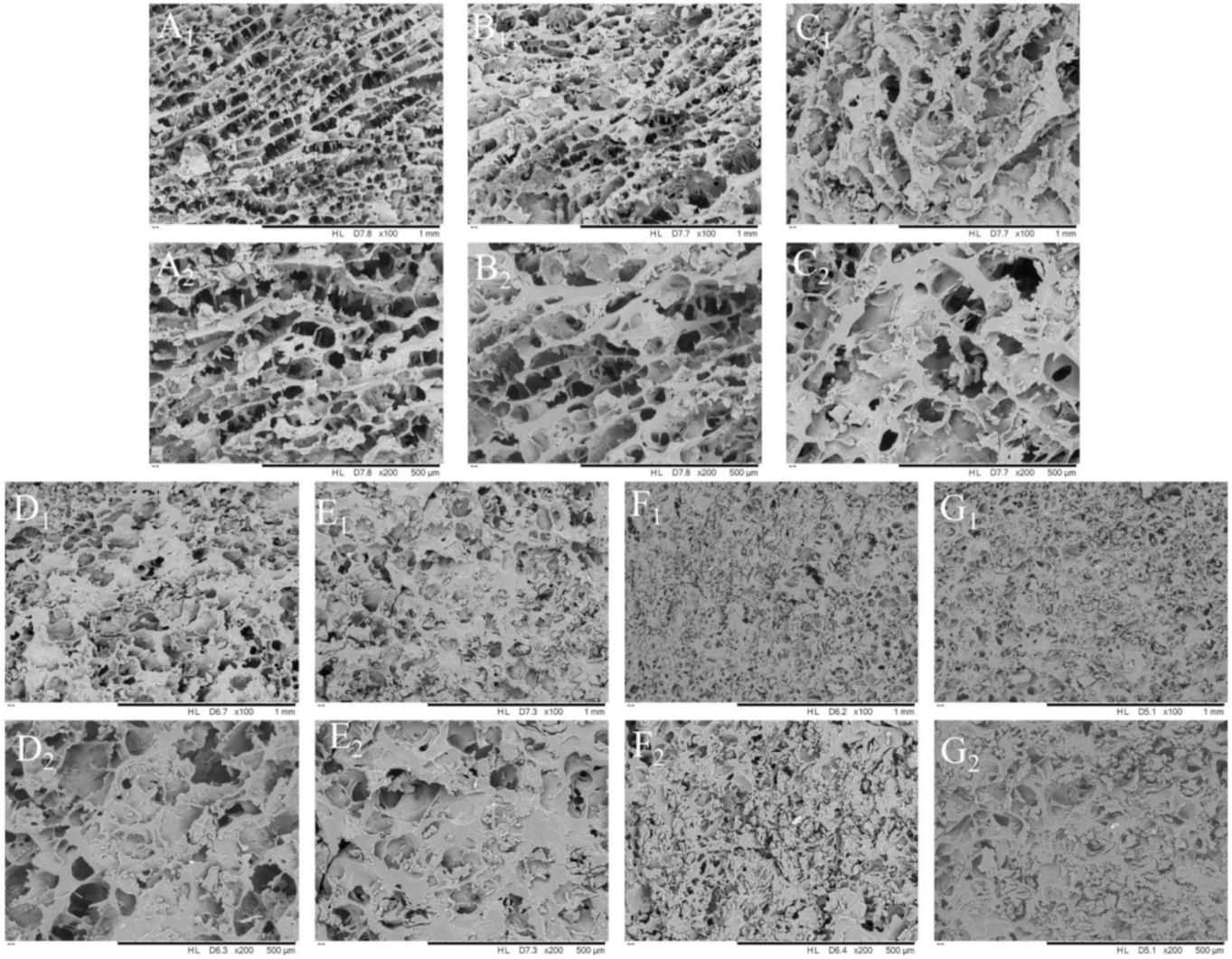

Fig. 9. SEM images from TFP-EWP-OJ composite gel with different CS concentrations. A_1-G_1 are SEM micrographs of TFP-EWP-OJ composite gel with CS concentrations of 0.00, 0.06, 0.08, 0.10, 0.12, 0.14, 0.16 g/mL at 100 magnification, respectively. A_2-G_2 are SEM micrographs of TFP-EWP-OJ composite gel with CS concentrations of 0.00, 0.06, 0.08, 0.10, 0.12, 0.14, 0.16 g/mL at 200 magnification, respectively. SEM: Scanning electron microscopy, TFP: Tremella polysaccharide, EWP: Egg white protein, OJ: Orange juice, CS: Corn starch.

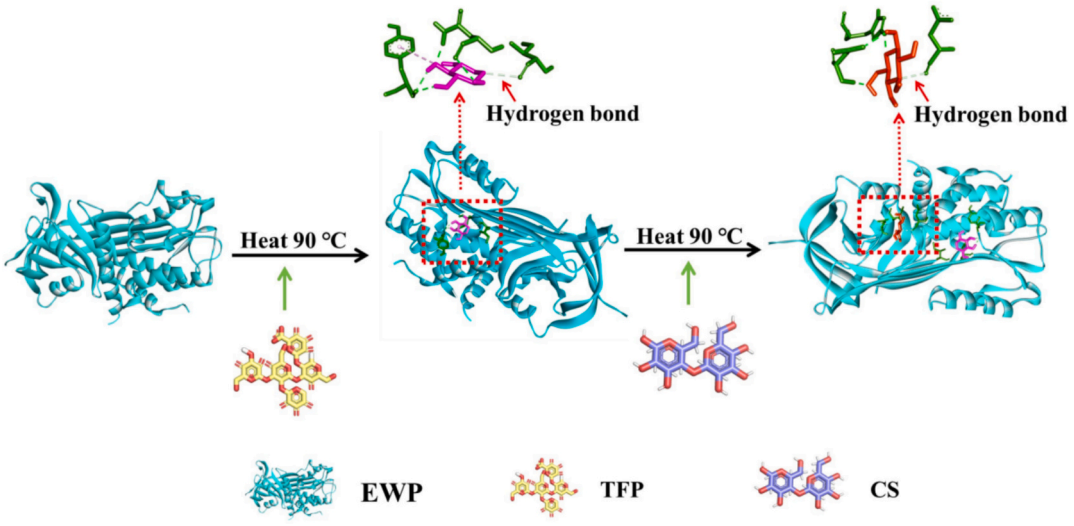

Fig. 10. Schematic representation of the formation mechanism of TFP-EWP-OJ composite gel. CS: Corn starch, TFP: Tremella polysaccharide, EWP: Egg white protein, OJ: Orange juice.

making extrusion difficult, which was not conducive to 3D printing (Fig. 1 F_1, $1F_2$, $1G_1$, and $1G_2$). As a result, the WHC of the material was not the greater, the better the print effects.

3.4. TPA

Textural properties are the main determinants of food acceptability, and it's also important for people with special needs (Yang et al., 2018). As shown in Fig. 7A, a gradual increase in hardness was found as the concentration of CS of the TFP-EWP-OJ composite gel increased ($P < 0.05$), which was consistent with the results for WHC. In addition, the TFP-EWP-OJ composite gel with 0.16 g/mL CS added had the highest hardness of 184.86 g. The gelatinized CS that formed in thermal induction process can be employed as filler materials to support the TFP-EWP-OJ composite gel network. The exertion of pressure on the protein phase through swelling action to enhanced the densification of the gel network (Hu et al., 2023). Consequently, the hardness of TFP-EWP-OJ composite gel was enhanced by the CS incorporation. This was beneficial for 3D printing. As shown in Fig. 7B, C, and D, the springiness, cohesiveness and gumminess of the TFP-EWP-OJ composite gel also gradually increased with increasing CS concentration. In particular, gumminess and cohesiveness were also favorable for 3D printing. This was due to high gumminess resulting in stronger adhesion between the layers and high cohesiveness resulting in a tighter internal structure, preventing deformation of the printed product. However, it can be seen from the 3D printing results that when the CS concentration was 0.12 g/mL, the TFP-EWP-OJ composite gel printing effect was the best. This indicated that materials with appropriate texture properties were more suitable for 3D printing.

3.5. FT-IR

Fig. 8 shown the FT-IR of TFP-EWP-OJ composite gel with different CS concentrations. It can reflect whether CS will have an effect on the characteristic functional groups of the TFP-EWP-OJ composite gel. As illustrated in Fig. 8, the infrared spectrum of the TFP-EWP-OJ composite gel with the incorporation of CS was comparable to the TFP-EWP-OJ composite gel without CS. Furthermore, no new absorption peaks were observed within the measured wavelength range. This suggested that no new functional groups were formed in the TFP-EWP-OJ composite gel after the addition of CS. However, with the increase in CS concentration, the peaks in the amide A band of the TFP-EWP-OJ composite gel were shifted towards the long wave direction from 3346 cm^{-1} to 3367 cm^{-1}. This was an indication that there were more hydrogen bonds between CS and TFP-EWP-OJ composite gel, reflecting the improved gel forming ability and gel strength of the composite system (Qian et al., 2023). This also meant that the printed material had greater deformation resistance and better self-supporting properties.

3.6. SEM

The microstructure of gel was very important for their physical properties. It can provide valuable theoretical support for structural changes during gel formation, particularly with regard to the homogeneity and densification of the gel network structure (Cao et al., 2012). The microstructures of TFP-EWP-OJ composite gel with different CS concentrations were illustrated in Fig. 9. It can be seen from the Fig. 9 A_1 and $9A_2$ that the microstructures of the TFP-EWP-OJ composite gel devoid of CS exhibited a lamellar network structure and a multitude of pores. The network structures of TFP-EWP-OJ composite gel with 0.06 g/mL and 0.08 g/mL CS became dense, but there were still large pores (Fig. 9 B_1, $9B_2$, $9C_1$, and $9C_2$). The number of pores on the surface of the TFP-EWP-OJ composite gel decreased gradually at CS concentrations of 0.10, 0.12, 0.14, and 0.16 g/mL, accompanied by a notable enhancement in microstructure compactness. This phenomenon may be attributed to the reaction of CS with EWP, which effectively inhibited the formation of excessive protein aggregates. Moreover this interaction became stronger as the CS concentration increases, making the network structure of the composite gel denser (Hu et al., 2023). The mechanical strength of the printed material was enhanced due to the increased density of the microstructure. Therefore, appropriate improvement of the microstructure of the printed material can improve the printing accuracy and resolution of the deposited layers, and the printed products will have a more stable structure and better dimensional stability (Mahdiyar et al., 2021).

3.7. TFP-EWP-OJ composite gel formation mechanism

CS could increase the elasticity, hardness, and WHC of the TFP-EWP-OJ composite gel. Furthermore, CS also made the network structure of the TFP-EWP-OJ composite gel more denser. Based on the FT-IR and intermolecular interactions, a general gelling mechanism for TFP-EWP-OJ composite gel is proposed. The explanation of the TFP-EWP-OJ composite gel-forming mechanism is when the protein is denatured by heating, the structure of the protein unfolds. Therefore, chemical groups such as sulfhydryl units, hydrophobic groups, and hydrogen bonding moieties are exposed within the protein (Wang et al., 2020). There are many hydroxyl groups in the structure of TFP and CS. After TFP and CS is added to the mixed system, they are subjected to chain cross-linking with EWP, in which they interact mainly through hydrogen bonds. Furthemore, a schematic representation of the formation mechanism of TFP-EWP-OJ composite gel is shown in Fig. 10.

4. Conclusion

The addition of CS had a significant effect on the 3D printing of TFP-EWP-OJ composite gel, rheological properties, WHC, TPA, and microstructure. The results showed that the printing accuracy of the TFP-EWP-OJ composite gel showed an increasing and then decreasing trend. Printed samples of TFP-EWP-OJ composite gels with 0.12 g/mL of CS had excellent self-supporting capabilities, delicate geometric shapes, and the highest printing accuracy. In addition, the nozzle diameter and printing speed suitable for 3D printing of TFP-EWP-OJ composite gel were 1.20 mm and 35 mm/s, respectively. The apparent viscosity of the TFP-EWP-OJ composite gel gradually decreased with increasing shear rate. This was indicative that the TFP-EWP-OJ composite gel had a shear thinning behaviour and was suitable to be applied to 3D printing. The apparent viscosity, G', G″, WHC, hardness, and springiness of the TFP-EWP-OJ composite gel were enhanced with the concentration of CS. This had a positive effect on the shape retention of the print samples. Furthermore, the microstructure of the TFP-EWP-OJ composite gel presented a gradual densification, accompanied by a reduction in pore size, with an increase in CS concentration. The results of FT-IR spectra demonstrated that no novel functional groups were generated between the CS and TFP-EWP-OJ composite gel. However, the interaction between the hydrogen bonds was found to be augmented. In conclusion, the study not only created a new printing material with high nutritional and multifunctional properties, but also provided an idea for the development of complex ink systems for other proteins.

CRediT authorship contribution statement

Lili Liu: Writing – review & editing, Writing – original draft, Supervision, Funding acquisition, Formal analysis, Conceptualization. **Beibei Shao:** Validation, Methodology, Formal analysis, Data curation, Conceptualization. **Wanlin Yang:** Software, Investigation. **Weiwei Cheng:** Supervision, Conceptualization. **Yue Ding:** Investigation. **Feng Xiao:** Validation, Investigation.

Declaration of competing interest

The authors declare that the research was conducted in the absence

of any commercial or financial relationships that could be construed as a potential conflict of interest.

Acknowledgements

This study was supported by National Key R&D Program of China (2024YFF1106202; 2022YFF1101600), Henan Province Science and Technology Research and Development (242102110092), Research Funding for Distinguished Professor at Henan University of Science and Technology (13510004), and the Leading Talent Program for Science and Technology Innovation in Central China (234200510020).

Data availability

Data will be made available on request.

References

An, Z. N., Liu, Z. B., Mo, H. Z., Hu, L. B., Li, H. B., Xu, D., & Chitrakar, B. (2023). Preparation of Pickering emulsion gel stabilized by tea residue protein/xanthan gum particles and its application in 3D printing. *Journal of Food Engineering, 343*, Article 111378. https://doi.org/10.1016/J.JFOODENG.2022.111378

Azam, R. M., Zhang, M., Bhandari, B., & Yang, C. H. (2018). Effect of different gums on features of 3D printed object based on vitamin-D enriched orange concentrate. *Food Biophysics, 13*(3), 250–262. https://doi.org/10.1007/s11483-018-9531-x

Cao, Y. Y., Xia, T. L., Zhou, G. H., & Xu, X. L. (2012). The mechanism of high pressure-induced gels of rabbit myosin. *Innovative Food Science and Emerging Technologies, 16*, 41–46. https://doi.org/10.1016/j.ifset.2012.04.005

Chen, Y. Y., Zhang, M., & Pattarapon, P. (2021). 3D printing of protein-based composite fruit and vegetable gel system. LWT-food. *Science and Technology, 141*, Article 110978. https://doi.org/10.1016/J.LWT.2021.110978

Costakis, W. J., Rueschhoff, L. M., Diaz-Cano, A. I., Youngblood, J. P., & Trice, R. W. (2016). Additive manufacturing of boron carbide via continuous filament direct ink writing of aqueous ceramic suspensions. *Journal of the European Ceramic Society, 36* (14), 3249–3256. https://doi.org/10.1016/j.jeurceramsoc.2016.06.002

He, W., Xiao, N. H., Zhao, Y., Yao, Y., Xu, M. S., Du, H. Y., … Y. G.. (2021). Effect of polysaccharides on the functional properties of egg white protein: A review. *Journal of Food Science, 86*(3), 656–666. https://doi.org/10.1111/1750-3841.15651

Hocine, S., Swygenhoven, H. V., Petegem, S. V., Chang, C. S. T., Maimaitiyili, T., Tinti, G., & Casati, N. (2020). Operando X-ray diffraction during laser 3D printing. *Materials Today, 34*, 30–40. https://doi.org/10.1016/j.mattod.2019.10.001

Hu, Y. Y., Chen, X., Cai, X. X., Zheng, Y. F., & Wang, S. Y. (2023). Effect of starch content and ultrasonic pretreatment on gelling properties of myofibrillar protein from Lateolabrax japonicus. *Food Frontiers, 4*(3), 1482–1495. https://doi.org/10.1002/FFT2.293

Li, G. H., Wang, B., Lv, W. Q., Mu, R. Y., & Zhong, Y. L. (2024a). Effect of induction mode on 3D printing characteristics of whey protein isolate emulsion gel. *Food Hydrocolloids, 146*, Article 109255. https://doi.org/10.1016/J.FOODHYD.2023.109255

Li, Y. L., Qi, X., Rong, L. Y., Li, J. W., Shen, M. Y., & Xie, J. H. (2024b). Effect of gellan gum on the rheology, gelling, and structural properties of thermally induced pea protein isolate gel. *Food Hydrocolloids, 147*, Article 109379. https://doi.org/10.1016/J.FOODHYD.2023.109379

Lim, W. S., Lim, N., Pake, H. J., & Lim, M. H. (2024). Emulsion gel-based 3D printable fat analogue prepared with pea protein isolate. *Journal of Food Engineering, 364*, Article 111801. https://doi.org/10.1016/J.JFOODENG.2023.111801

Lin, Q. Z., Shang, M. S., Li, X. J., Sang, C. Y., Chen, L., Long, J., … Z. Y.. (2024). Rheology and 3D printing characteristics of heat-inducible pea protein-carrageenan-glycyrrhizic acid emulsions as edible inks. *Food Hydrocolloids, 147*, Article 109347. https://doi.org/10.1016/J.FOODHYD.2023.109347

Liu, L. L., Yang, X. P., Bhandari, B., Meng, Y. Y., & Prakash, S. (2020). Optimization of the formulation and properties of 3D-printed complex egg white protein objects. *Foods, 9* (2), 164. https://doi.org/10.3390/foods9020164

Liu, Z. B., Bhandari, B., Prakash, S., Mantihal, S., & Zhang, M. (2019). Linking rheology and printability of a multicomponent gel system of carrageenan-xanthan-starch in extrusion based additive manufacturing. *Food Hydrocolloids, 87*, 413–424. https://doi.org/10.1016/j.foodhyd.2018.08.026

Liu, Z. B., Chen, X., Dai, Q. Y., Xu, D., Hu, L. B., Li, H. B., … H. Z.. (2023). Pea protein-xanthan gum interaction driving the development of 3D printed dysphagia diet. *Food Hydrocolloids, 139*, Article 108497. https://doi.org/10.1016/J.FOODHYD.2023.108497

Liu, Z. B., Ha, S. Y., Guo, C. F., Xu, D., Hu, L. B., Li, H. B., & Mo, H. Z. (2024). 3D printing of curcumin enriched Pickering emulsion gel stablized by pea protein-carrageenan complexes. *Food Hydrocolloids, 146*, Article 109170. https://doi.org/10.1016/J.FOODHYD.2023.109170

Liu, Z. B., Zhang, M., & Bhandari, B. (2018b). Effect of gums on the rheological, microstructural and extrusion printing characteristics of mashed potatoes. *International Journal of Biological Macromolecules, 117*, 1179–1187. https://doi.org/10.1016/j.ijbiomac.2018.06.048

Liu, Z. B., Zhang, M., Bhandari, B., Yang, C., & H.. (2018a). Impact of rheological properties of mashed potatoes on 3D printing. *Journal of Food Engineering, 220*, 76–82. https://doi.org/10.1016/j.jfoodeng.2017.04.017

Ma, X., Yang, M., He, Y., Zhai, C. T., & Li, C. L. (2021). A review on the production, structure, bioactivities and applications of tremella polysaccharides. *International Journal of Immunopathology and Pharmacology, 35*, 1–14. https://doi.org/10.1177/20587384211000541

Mahdiyar, S., Henry, J., Chen, J. S., & Rammile, E. (2021). Construction of 3D printed reduced-fat meat analogue by emulsion gels. Part II: Printing performance, thermal, tribological, and dynamic sensory characterization of printed objects. *Food Hydrocolloids, 121*, Article 107054. https://doi.org/10.1016/J.FOODHYD.2021.107054

Nailín, C. M., Gipsy, T. M., Mario, P. W., Carolina, H. L., Roberto, L. M., & Luis, M. O. (2023). Evaluation of physicochemical properties of starch-protein gels: Printability and postprocessing. LWT-food. *Science and Technology, 182*, Article 114797. https://doi.org/10.1016/J.LWT.2023.114797

Pan, Y. M., Sun, Q. X., Liu, Y., Wei, S., Xia, Q. Y., Zheng, O. Y., … J. M.. (2021). The relationship between rheological and textural properties of shrimp surimi adding starch and 3D printability based on principal component analysis. *Food Science & Nutrition, 9*(6), 2985–2999. https://doi.org/10.1002/FSN3.2257

Phuhongsung, P., Zhang, M., & Devahastin, S. (2020). Investigation on 3D printing ability of soybean protein isolate gels and correlations with their rheological and textural properties via LF-NMR spectroscopic characteristics. LWT-food. *Science and Technology, 122*, Article 109019. https://doi.org/10.1016/j.lwt.2020.109019

Qian, Z., Dong, S. Z., Zhong, L., Zhan, Q. P., Hu, Q. H., & Zhao, L. Y. (2023). Effects of carboxymethyl chitosan on the gelling properties, microstructure, and molecular forces of Pleurotus eryngii protein gels. *Food Hydrocolloids, 145*, Article 109158. https://doi.org/10.1016/J.FOODHYD.2023.109158

Ren, S. N., Tang, T., Bi, X. F., Liu, X. C., Xu, P. K., & Che, Z. M. (2023). Effects of pea protein isolate on 3D printing performance, nutritional and sensory properties of mango pulp. Food. *Bioscience, 55*, Article 102994. https://doi.org/10.1016/J.FBIO.2023.102994

Shao, B. B., Liu, L. L., Zhang, N., Cheng, W. W., Ding, Y., Xiao, F., & Wang, Y. T. (2025). Effect of Tremella fuciformis polysaccharide on gel properties and structure of egg white protein. *Food and Fermentation Industries, 8*. https://doi.org/10.13995/j.cnki.11-1802/ts.039610

Sheng, L., Wang, Y., Chen, J., Zou, J., Wang, Q., & Ma, M. (2018). Influence of high-intensity ultrasound on foaming and structural properties of egg white. *Food Research International, 108*, 604–610. https://doi.org/10.1016/j.foodres.2018.04.007

Shi, H. M., Li, J., Xu, E. B., Yang, H. Y., Liu, D. H., & Yin, j.. (2023). Microscale 3D printing of fish analogues using soy protein food ink. *Journal of Food Engineering, 347*, Article 111436. https://doi.org/10.1016/j.jfoodeng.2023.111436

Teixeira, A. S., Deladino, L., García, M. A., Zaritzky, N. E., Sanz, P. D., & Molina-García, A. D. (2018). Microstructure analysis of high pressure induced gelatinization of maize starch in the presence of hydrocolloids. *Food and Bioproducts Processing, 112*, 119–130. https://doi.org/10.1016/j.fbp.2018.09.009

Wang, W. J., Shen, M. Y., Jiang, L., Song, Q. Q., Liu, S. C., Xie, J. H., et al. (2020). Influence of Mesona blumes polysaccharide on the gel properties and microstructure of acid-induced soy protein isolate gels. *Food Chemistry, 313*, Article 126125. https://doi.org/10.1016/j.foodchem.2019.126125

Wang, X., Zhang, M. S. M. A., & Li, J. Y. (2023). Easy-to-swallow mooncake using 3D printing: Effect of oil and hydrocolloid concentration. *Food Research International, 164*, Article 112404. https://doi.org/10.1016/J.FOODRES.2022.112404

Wang, Z. M., Chen, F. N., Deng, Y. Y., Tang, X. J., Li, P., Zhao, Z. H., … G.. (2024). Texture characterization of 3D printed fibrous whey protein-starch composite emulsion gels as dysphagia food: A comparative study on starch type. *Food Chemistry, 458*, Article 140302. https://doi.org/10.1016/J.FOODCHEM.2024.140302

Xu, B. G., Wang, X. D., Chitrakar, B., Xu, Y., Wei, B. X., Wang, B., … H. L.. (2025). Effect of various physical modifications of pea protein isolate (PPI) on 3D printing behavior and dysphagia properties of strawberry-PPI gels. *Food Hydrocolloids, 158*, Article 110498. https://doi.org/10.1016/J.FOODHYD.2024.110498

Yang, F. L., Zhang, M., Bhandari, B., & Liu, Y. P. (2018). Investigation on lemon juice gel as food material for 3D printing and optimization of printing parameters. *LWT- Food Science and Technology, 87*, 67–76. https://doi.org/10.1016/j.lwt.2017.08.054

Yu, J., Li, D., Wang, L. J., & Wang, Y. (2023). Improving freeze-thaw stability and 3D printing performance of soy protein isolate emulsion gel inks by guar & xanthan gums. *Food Hydrocolloids, 136*, Article 108293. https://doi.org/10.1016/J.FOODHYD.2022.108293

Zhang, D., Chen, L., Cai, J., Dong, Q., Din, Z. U., Hu, Z. Z., & Cheng, S. Y. (2021). Starch/tea polyphenols nanofibrous films for food packaging application:From facileconstruction to enhance mechanical, antioxidant and hydrophobic properties. *Food Chemistry, 360*, Article 129922. https://doi.org/10.1016/J.FOODCHEM.2021.129922

Zheng, L. Y., Li, D., Wang, L. J., & Wang, Y. (2024). Tailoring 3D-printed high internal phase emulsion-rice starch gels: Role of amylose in rheology and bioactive stability. *Carbohydrate Polymers, 331*, Article 121891. https://doi.org/10.1016/J.CARBPOL.2024.121891

Zhu, Y. L., Chen, L., Zhang, X. F., Meng, T., Liu, Z. B., Bimal, C., & He, C. J. (2023). 3D-printed pea protein–based dysphagia diet affected by different hydrocolloids. *Food and Bioprocess Technology, 17*(6), 1492–1506. https://doi.org/10.1007/S11947-023-03210-1